JCTC Journal of Chemical Theory and Computation

Potential Energy Surface Profile of the Oxygen Reduction Reaction on a Pt Cluster: Adsorption and Decomposition of OOH and H_2O_2

Yixuan Wang* and Perla B. Balbuena*

Department of Chemical Engineering, Texas A&M University, 3122 TAMU, College Station, Texas 77843

Received March 26, 2005

Abstract: Because of their essential roles on determining pathways of the oxygen reduction reaction (ORR), the adsorption behavior and decomposition of the radical OOH and hydrogen peroxide on Pt clusters (Pt_n, $n = 3$, 6, and 10) are extensively investigated using density functional theory. Two types of adsorption of the radical OOH on Pt clusters are found. One-end adsorbed hydrogen peroxide H_2O_2, arising from reduction of adsorbed OOH, is also located on Pt_3, with an adsorption energy of −0.63 eV, suggesting that the ORR may proceed via a series pathway generating H_2O_2 as an intermediate. However, since OOH readily decomposes on Pt_3 into atop adsorbed atomic oxygen and hydroxyl with an activation energy of only ∼0.25 eV, the OOR may take place preferentially via a direct pathway without H_2O_2 produced. A potential energy surface profile for the ORR is proposed, and the adsorption properties of other involved oxide species are characterized.

1. Introduction

The oxygen reduction reaction (ORR), taking place at the cathode of polymer-electrolyte-membrane fuel cells (PEMFC), has been attracting much attention[1−7] in the recent decades because of the desire to elucidate its slow kinetics on electrocatalyst surfaces, which is one of the bottlenecks for achieving improved efficiencies in the fuel cell operation.[8] On the other hand, understanding the ORR mechanisms on a Pt(111) surface, currently known as one of the most active electrocatalysts of PEMFCs, undoubtedly has also significant implications to designing alternative cathode catalysts, aiming to decrease the required amount of the expensive noble metal and to improve the ORR reaction kinetics.

The *overall* ORR on Pt surfaces is a multielectron complex reaction that includes a number of elementary reactions. Yeager proposed two pathways for the *overall* OER in acid medium:[2] (a) a *direct* 4-electron pathway where O_2 is reduced directly to water without involvement of hydrogen peroxide (H_2O_2), $O_2 + 4H^+ + 4e^- \rightarrow 2H_2O$, and (b) a *series* pathway in which O_2 is reduced to H_2O_2, $O_2 + 2H^+ + 2e^- \rightarrow H_2O_2$, followed by its further reduction, $H_2O_2 + 2H^+ + 2e^- \rightarrow 2H_2O$. It was thereafter suggested that the O_2 reduction on a Pt surface proceeds by a *parallel* pathway, the *direct* and *series* mechanisms occurring simultaneously, with the *direct* as the dominant one.[3] Recent studies from Marković et al.[9] somewhat favored and suggested that a *series* pathway via an *adsorbed* H_2O_2 intermediate may apply to Pt and Pt-based bimetallic catalysts.

Quantum mechanics provides an alternative way to explore the ORR, which is a good complement to state-of-the-art experimental techniques. Using a single Pt atom[5] and two Pt atoms (Pt_2)[6] to coordinate the species most likely to be found on the potential energy surface of the ORR, Anderson and co-workers extensively analyzed the mechanism of the ORR at a molecular level. Adsorbed OOH was proposed as an intermediate for the first electron-transfer step, and its formation has a lower activation energy than the dissociation of the adsorbed O_2 (0.6 eV vs 0.7 eV), implying that O_2 may not dissociate on the Pt surface before the first electron transfer. They also found that OOH dissociation on Pt has a rather small activation barrier of ∼0.06 eV. Our Car-Parrinello molecular dynamics (CPMD) simulations of the ORR on a Pt(111) surface in the presence of hydrated protons

* Corresponding author e-mail: yixuan.wang@chemail.tamu.edu (Y.W.) and balbuena@tamu.edu (P.B.B.).

10.1021/ct0500794 CCC: $30.25
Published on Web 08/06/2005

at 350K basically support their findings.[10] Although dissociative adsorption of O_2 may take place, the adsorbed O_2 would combine with the transferred proton to form OOH_{ads} rather than decompose. Also, OOH_{ads} readily decomposes and is unable to yield H_2O_2. These findings seem to be inconsistent with those from experiments indicating that a certain amount (0−20%, depending on the applied potential) of hydrogen peroxide is formed as either a product or an intermediate of the ORR on Pt(111) surfaces.[11,12] A slight attempt is made here to review the previous work in detail, but it is necessary to mention that there is still a lack of agreement with respect to the nature of the overall ORR mechanism, which motivates us to carry out the present investigation.

A variety of intermediates can be present in the process of the ORR, such as atomic O, radicals OH and OOH, and H_2O_2. The adsorption properties of these intermediates on the Pt electrode are therefore very important to obtain insights into the ORR mechanism. Balbuena et al. investigated O, OH, and H_2O adsorption on Pt and Pt-based bimetallic clusters.[13] Using planewave-based periodic density functional theory, Panchenko et al.[14] very recently performed systematic calculations for adsorption behavior of ORR intermediates on low-index Pt surfaces. In the present study, we first focus on adsorption and decomposition of OOH and H_2O_2 on Pt clusters. The properties of the transition states for the decomposition of H_2O_2 on Pt clusters are reported for the first time to the best of our knowledge. Then, coadsorptions of the relevant oxides are systematically investigated, e.g., O/OH, O/H_2O, OH/OH, OH/H_2O, and H_2O/H_2O. On the basis of this information, a potential energy surface profile of the ORR is established, which allows discussing a couple of very important issues about the reaction mechanisms of the ORR. Individual adsorptions on Pt clusters of some relevant species have been previously investigated by DFT, including O, OH, O_2, and H_2O on Pt_2, Pt_3, and bigger clusters,[6,13−17] for the sake of self-consistency, particularly with respect to necessary corrections, like zero point energy (ZPE) and basis set superposition error (BSSE) corrections; we also did our own calculations for adsorptions of O, OH, O_2, and H_2O on Pt_3.

2. Computational Details

Geometries were fully optimized with the hybrid B3LYP density functional[18,19] as implemented in Gaussian03 RevC.02[20] together with the LANL2DZ pseudopotential and the corresponding double-ζ basis set for Pt[21] and with the 6-311++G** basis set for oxygen and hydrogen. The S^2 expectation values for the involved open-shell species with B3LYP are nearly identical to the exact value, indicating that B3LYP is proper to treat the present open shell systems. The relevant transition states were located with conventional linear synchronous transit QST2 or quadratic synchronous transit QST3 methods. To characterize the stationary points and make the zero point energy (ZPE) corrections, a frequency analysis was done for all stationary points at this level. All minima and transition states have the proper number of imaginary frequencies. To explicitly establish the relevant species, the intrinsic reaction coordinate (IRC) pathway was also run for all the transition states presented here. Since the default grid for the integral did not give sufficient numerical accuracy for some calculations, causing convergence difficulties, "ultrafine" grid was used in all of the present DFT calculations. If not noted otherwise, adsorption energies in the text usually refer to values with unscaled ZPE correction. BSSE corrections were estimated for some complexes.[22] The results show that BSSE is not significant at the level of B3LYP/6-311++G**. For example, BSSE corrections for adsorption energies of O, H_2O, and H_2O_2 on Pt_3 are 0.06, 0.08, and 0.08 eV, respectively. Refined energies were attempted with a sophisticated electron correlation method, CCSD(T), for all of the B3LYP-optimized structures, yet they failed for a few open shell complexes probably due to too high spin contamination.

3. Results and Discussion

3.1. Adsorptions of O, OH, O_2, and H_2O on Pt_3. Consistent with a sophisticated ab initio method, relativistic CI calculation including spin−orbit effects,[23] the present optimization of Pt_3 finds that the triplet state $^3B_1$ (C_{2v} symmetry with Pt−Pt bond lengths of 2.499 and 2.583 Å) is the ground state yet is almost degenerate with the singlet state $^1A_1$ (D_{3h} symmetry with Pt−Pt bond lengths of 2.521 Å) by a small energy difference of 0.011 eV. A very recent B3LYP calculation with Pt−Pt bond lengths fixed at 2.775 Å also predicted that the triplet state is the ground state of Pt_3.[17] Despite small differences arising from the employed methods and calculation details, adsorption energies and sites of the oxide species on Pt_3 are in reasonable agreement between the present and previous results, which are summarized in Table 1. Adsorption energies are defined as the difference between the energy of the complex (e.g., Pt_3−O) and the sum of the energies of the adsorbate (O) and adsorbent (Pt_3). O is most stably adsorbed on a bridge site with a singlet ground state and an adsorption energy of −3.10 eV, closely followed by a top adsorption with a triplet ground state and an adsorption energy of −3.06 eV. The OH radical is preferentially adsorbed atop on Pt_3 with an adsorption energy of −2.62 eV. Previous theoretical studies[14,24] show that OH strongly binds on top as well as on the bridge site of Pt(111) with an adsorption energy between −2.14 and −2.52 eV at low coverage. The adsorption of H_2O on Pt_3 (adsorption energy ∼0.6 eV) with a closed electronic shell is much weaker than those of O and OH; however, it is still one time stronger than regular hydrogen bonding.

3.2. •OOH Adsorption and Dissociation on Pt_n (n = 3, 4, 6, and 10). Two types of •OOH adsorption on Pt_3 have been located. As shown in Figure 1, the structure **S1** is most likely to be considered as a 1-fold adsorption with oxygen connecting to Pt, and structure **S2** is a 2-fold adsorption with Pt−O shorter than Pt−O(H) (2.017 vs 2.418 Å). Adsorption energies of OOH to Pt_3 in **S1** and **S2** are −1.64 and −1.26 eV, respectively. **S2** corresponds to the bridge adsorption conformer of •OOH on Pt(111) reported by Panchenko et al.,[14] where the Pt−O bond distances are 2.03 and 2.64 Å with an adsorption energy of −1.07 eV. Mulliken population analysis indicates that the charge is transferred from the Pt_3 cluster to •OOH by 0.38 and 0.20e in **S1** and **S2**, respectively. Specifically, the charge is mostly transferred from *d* orbitals of the Pt atoms to *p* orbitals of oxygen. The strong adsorption

Table 1. Adsorption and Coadsorption Properties of Oxides on Pt_3: Adsorption Energies (AE/eV), Distances between Pt and O unless Those Noted for O−O, and Vibrational Frequencies of Pt−O Stretch unless Those Specified for O−O Stretch

system	multiplicity	adsorption site[a]	−AE,[b] present	−AE, references	distances/Å	vibrational frequency/ cm^{-1}
O	1	top	2.90/2.98	2.812[f]	1.753	861
	3	top	3.06/3.12	3.455,[f]3.22[c]	1.787	763
	1	bridge	3.10/3.17	3.269,[f]3.24[c]	1.918, 1.918	619
	3	bridge	2.81/2.87		1.960, 1.959	566
OH	2	top	2.62/2.74	2.92[c]	1.943	584
	4	bridge	1.93/2.07	2.10[c]	2.203, 2.203	398
				2.23 (atop),[g] 2.14(bridge)[g]		
O_2	1	bridge	0.02	0.58;[d]	2.08, 1.316(O−O)	541, 1052(O−O)
	3	bridge	0.56/0.60	1.08;[d]	2.102, 2.102, 1.318(O−O)	538, 1050(O−O)
				0.4−0.5[e]		
				0.63(bridge)[g]		
H_2O	1	top	0.64	1.02;[c]	2.25	293
OOH	2	top	1.57/1.64	1.07[g]	1.954, 1.420(O−O)	504 , 896(O−O)
		bridge	1.18/1.26		2.017, 2.482, 1.461(O−O)	492, 781(O−O)
O/OH	2	top	5.41		1.753, 1.932	837/597
	4	top	5.62		1.794, 1.934	749/597
H_2O_2	1	top	0.67		2.150, 1.495(O−O)	660(O−O)
OH/OH	1	top	4.92		1.922, 1.922	598
	3	top	5.21		1.929,1.938	592
O/H_2O	1	top	3.20		1.759, 2.232	849, 308
	3	top	3.86		1.784, 2.213	778, 314
OH/H_2O	2	top	3.32		1.953, 2.233	560, 303
H_2O/H_2O	1	top	1.27		2.257, 2.242	299

[a] Top: one site, with a Pt atom directly connecting to O atom; bridge, O bridges two Pt atoms. [b] AE = *E*(complex) − *E*(Pt_3,M=3) - *E*(adsorbate), separated by a slash they refer to those with and without ZPE. [c] Reference 13, full optimization using B3PW91 with LANL2DZ for Pt and 6-31G* for O implemented in Gaussian 98. [d] Reference 16. [e] Experimental.[28] [f] Reference 17, B3LYP with LANL ECP and LACVP** basis set for Pt and 6-31G** for O, Pt−Pt is fixed at 2.775 Å. [g] Reference 14, VASP (PW91-GGA/PAW) results for a four-layer Pt(111) slab.

of •OOH to Pt_3 is also reflected by a O−O vibrational frequency shift of 259 cm^{-1} in **S1** as compared with the naked •OOH (896 vs 1155 cm^{-1}), as well as by O−O bond stretching of approximately 0.1 Å (1.424 in **S1** vs 1.328 Å in •OOH).

B3LYP predicts that the distorted tetrahedron with a triplet state is the ground state for Pt_4. According to Table 2, the corresponding adsorption of OOH (**S1′**) on the Pt_4 cluster has a similar strength to that on Pt_3 (−1.67 vs −1.57 eV). The ground state of planar Pt_6 with Pt−Pt bond lengths fixed

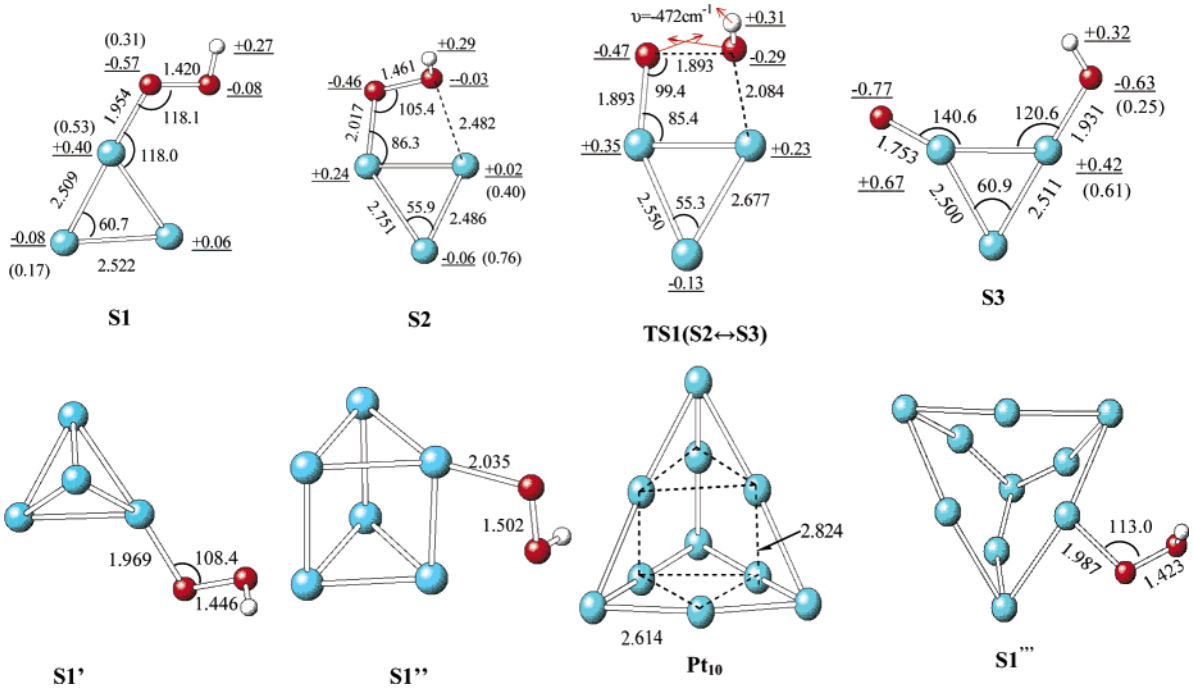

Figure 1. B3LYP optimized structures; bond lengths (in Å) and angles (°) are displayed. The underlined data are Mulliken charges, and those in parentheses are spin densities.

Table 2. Spin Multiplicity (*M*) of Complexes, Distances (R/Å) between Adsorbed Oxygen and Pt, and Adsorption Energies (ΔE/eV) of OOH and H_2O_2 on Pt Clusters Calculated with B3LYP

	Pt	Pt_2	Pt_3	Pt_4	Pt_6	Pt_{10}
			OOH			
M	2	2	2	2	2	8
R	Pt−O=1.882	Pt−O=1.941	Pt−O=1.954	Pt−O=1.969	Pt−O=2.035	Pt−O=1.987
	O−O=1.443	O−O=1.483	O−O=1.420	O−O=1.446	O−O=1.502	O−O=1.423
ΔE	−1.63	−1.42	−1.57	−1.67	−1.92	−1.18
			H_2O_2			
M	1	3	1	3	3	9
R	Pt−O=2.011	Pt1−Pt2=2.381	Pt1−Pt2=2.521	Pt1−Pt2=2.665	Pt1−Pt2=2.675	Pt1−Pt2=2.683
	O−O=1.523	Pt2−O=2.269	Pt1−O=2.173	Pt1−O=2.280	Pt1−O=2.234	Pt1−O=2.436
		O−O=1.460	O−O=1.495	O−O=1.460	O−O=1.465	O−O=1.455
				H−Pt2=2.840	H−Pt2=2.632	H−Pt2=2.575
ΔE	−0.43	−0.58	−0.67	−0.52	−0.44	−0.36

at 2.776 Å is a high spin state (multiplicity, M=7).[17] 1-fold adsorption of OOH on Pt_6 (M=6) was located yet with a lower adsorption energy of −0.86 eV. Two Pt_6 clusters, a singlet distorted octahedron and a triplet prism, were optimized, the latter having lower energy than the former by 1.02 eV. The adsorption energy of OOH on the Pt_6 prism is approximately −1.92 eV (**S1″**). The fully optimized Pt_{10} cluster shows that Pt−Pt bond lengths are different, 2.614 Å between a corner atom and an edge atom and 2.823 Å between two edge atoms. The ground state of Pt_{10} possesses high multiplicity of M = 9, and the electronic configuration for T_d-constrained Pt_{10} is $t_1^2e^2a_1t_2^3$, leading to no Jahn−Teller effect. Thus, the Pt_{10} cluster maintains T_d symmetry. The adsorption species (**S1‴**, M=8 for the ground state; adsorption energy ∼ −1.18 eV) of OOH on Pt_{10}, corresponding to **S1** of OOH on Pt_3, has also been located.

The dissociation of the superoxide radical can be catalyzed by a Pt cluster. A transition state (**TS1**) for the dissociation of **S2** has been characterized by the vibrational mode of its unique imaginary frequency (∼473 cm^{-1}) as well as by IRC analysis, as illustrated in Figure 2 that displays the electronic structure energy (relative to the reactant) against the O−O distance. The activation energy for the dissociation of **S2** into coadsorbed O and OH on Pt_3 (**S3**) is ∼0.25 eV. The dissociation of **S2** is most probably driven by the adsorption of the radical OH on Pt_3, causing a significant energy decrease of ∼1.5 eV from **S2** to **S3**. Sidik et al. obtained an activation energy of 0.06 eV for •OOH dissociation on Pt_2 with the Pt−Pt distance fixed at 2.77 Å and estimated that the activation energy increased to 0.15 eV using the same transition state structure as Pt_2−OOH over a two-layer Pt_{15}.[6] No other information on the dissociation of the peroxide radical has been reported. O and OH are quite separated at two top sites in **S3**, and the ground state is quartet (M=4) with an adsorption energy of −5.62 eV, which is rather similar to the sum of that of O (top with triplet ground state, −3.06 eV) and of OH (top with doublet ground state, −2.62 eV).

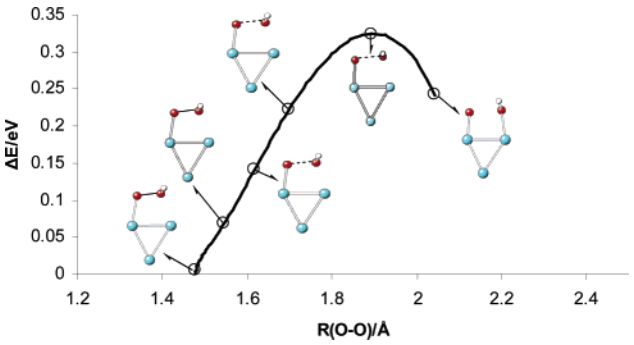

Figure 2. Relative electronic energy (in eV) against O−O distance (in Å) obtained with IRC analysis for the transition state TS1.

The preexponential factor A for the decomposition of adsorbed OOH, estimated by conventional transition-state theory, is 1.1×10^{11} s^{-1}.

3.3. H_2O_2 Adsorption and Dissociation on Pt_3. Hydrogen peroxide, H_2O_2, is usually proposed as either a product or an intermediate of the oxygen reduction reaction on Pt surfaces.[11,12] A 1-fold adsorption conformer through oxygen is located for H_2O_2 on Pt_3 (**S4,** Figure 3), but a 2-fold adsorption, i.e., bridge adsorption, was not found. Starting with a geometry close to bridge adsorption, the geometry optimization always yield two coadsorbed hydroxyls. The binding energy of H_2O_2 to Pt_3 is only ∼ −0.67 eV, which is considerably less than those of the radicals, O (−3.1), OH (−2.6), and OOH (−1.6), and the Pt−O distances of 2.173 Å are greater than those in such complexes as Pt_3−O (∼1.787 Å, top adsorption), Pt_3−OH (1.943 Å), and Pt_3−OOH (1.954 Å). Despite the weak adsorption of **S4**, as compared with naked H_2O_2, the O−O bond length is still stretched by 0.04 Å (1.495 vs 1.454 Å) with an O−O vibrational frequency shift of 273 cm^{-1} (660 vs 933 cm^{-1}). Despite the lower adsorption energies (−0.52, −0.50, and −0.36 eV), such weak adsorbed species of H_2O_2 (**S4′**, **S4″**, and **S4‴**) have also been located on Pt_4, Pt_6, and Pt_{10}, as shown in Figure 3. Panchenko et al. tried to locate the adsorption species of H_2O_2 on Pt(111), (100), and (110) surfaces, but they claimed that H_2O_2 was unstable and dissociated into two adsorbed hydroxyls.[14] Adsorbed H_2O_2 on Pt-polycrystalline has been frequently suggested as the intermediate of the ORR by experimentalists;[25] however, direct measurement or other theoretical calculations on large clusters or extended Pt surfaces have not been reported. According to Table 2, adsorption energies of H_2O_2 on the Pt_n (n=1−10) clusters

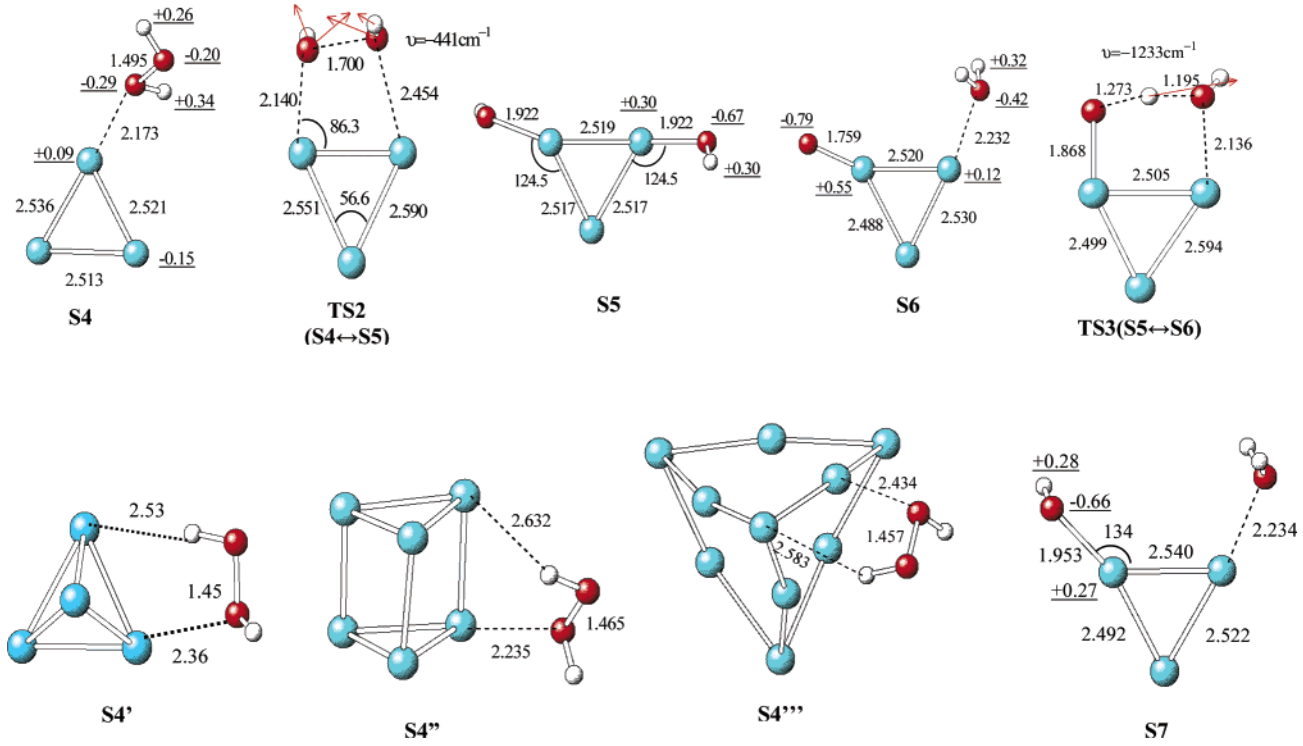

Figure 3. B3LYP optimized structures; bond lengths (in Å) and angles (°) are displayed. The underlined data are Mulliken charges.

are in the range from −0.36 to −0.67 eV. Especially, adsorption strengths of H_2O_2 on Pt_6 and Pt_{10} are very similar. Thus, it is hard to believe that the adsorption of H_2O_2 will cease as the size of the Pt cluster grows to an extended surface. However, the adsorption of H_2O_2 on Pt is still an opening question that needs to be further investigated.

A transition state (**TS2**) for the dissociation of the one-end adsorbed H_2O_2 (**S4**) into two coadsorbed hydroxyls is illustrated in Figure 3, and the activation energy is ∼0.57 eV. The O−O bond length in **TS2** is stretched to 1.7 Å. IRC analysis confirms that **TS2** connects **S4** and two coadsorbed hydroxyls on Pt_3, i.e., **S5**. **S5** is much more stable than **S4** by 2.73 eV, suggesting that the dissociation of **S4** is primarily driven by the strong adsorption of the hydroxyl radical. The preexponential factor *A* for the decomposition of **S4** estimated by transition-state theory is 1.7×10^{11} s^{-1}. The ground state of **S5** is a triplet, and its adsorption energy (−5.21 eV) is almost twice of that of OH to Pt_3, indicating that adsorption of two coadsorbed hydroxyls have a negligible cooperative effect.

Since H_2O_2 may dissociate on a Pt surface into water and oxygen,[26] and •OOH for the first reduction step of O_2 may be reduced to O and H_2O,[5] the coadsorption of O and H_2O on Pt_3 is also investigated, designated as **S6** in Figure 3. The ground state of **S6** has the same spin as the adsorbed O, triplet state, and its adsorption energy of −3.86 eV (taking O, H_2O, and triplet Pt_3 as references) is rather close to the sum of O (−3.06 eV for top adsorption) and H_2O (−0.64 eV). The thermodynamic stability of **S6** lies between **S4** (H_2O_2−Pt_3) and **S5** (2HO−Pt_3), i.e., the energy of **S6** is lower by 1.90 eV than **S4** and higher by 0.83 eV than **S5**. The proton transfer between **S5** and **S6** could be carried out via the transition state (**TS3**), in which the proton is shared by the oxygen and the hydroxyl oxygen. The activation energy from **S6** to **S5** is only ∼0.15 eV, and that of the reverse H transfer is 0.68 eV. The relatively lower energy barrier (∼0.15 eV, ∼3−4 kcal/mol) of the proton transfer from **S5** to **S6** indicates that the proton transfer can take place at room temperature.

3.4. Coadsorptions of OH/H_2O and H_2O/H_2O on Pt_3. As the possible products from the third and forth reduction steps of oxygen, coadsorbed OH/H_2O (**S7**) and H_2O/H_2O (**S8**, not shown) on Pt_3 are also optimized. Pt−O distances in **S7** are very similar to their individual complexes of OH and H_2O (1.953 vs 1.943 Å; 2.234 vs 2.254 Å), and the adsorption energy of −3.32 eV is consequently almost the sum of OH (∼2.62 eV) and H_2O (∼0.64) on Pt_3. Likewise, negligible cooperativity was found for H_2O/H_2O coadsorption, in which an adsorption energy of −1.27 eV is nearly twice that of a single H_2O on Pt_3.

3.5. Potential Energy Surface Profile of the ORR on Pt_3 Cluster. Starting with the adsorption of O_2 to Pt_3, and assuming that the adsorbed oxygen species reacts directly with a proton from the electrolyte, the potential energy surface profile for ORR has been illustrated in Figure 4 on the basis of the energies of the relevant species and available activation energies for a few key reactions. For the benefit of readers who are more familiar with electrochemical discussions of this topic, the energetics of the ORR is also given in Figure 5 referring to the standard hydrogen electrode potential as presented by Anderson and Albu.[29] We note that although the reaction mechanism may quantitatively depend on a number of factors, including electrode potential, electrolyte, and adsorbate coverage, the main features of the ORR may be qualitatively provided by cluster-based DFT calculations.

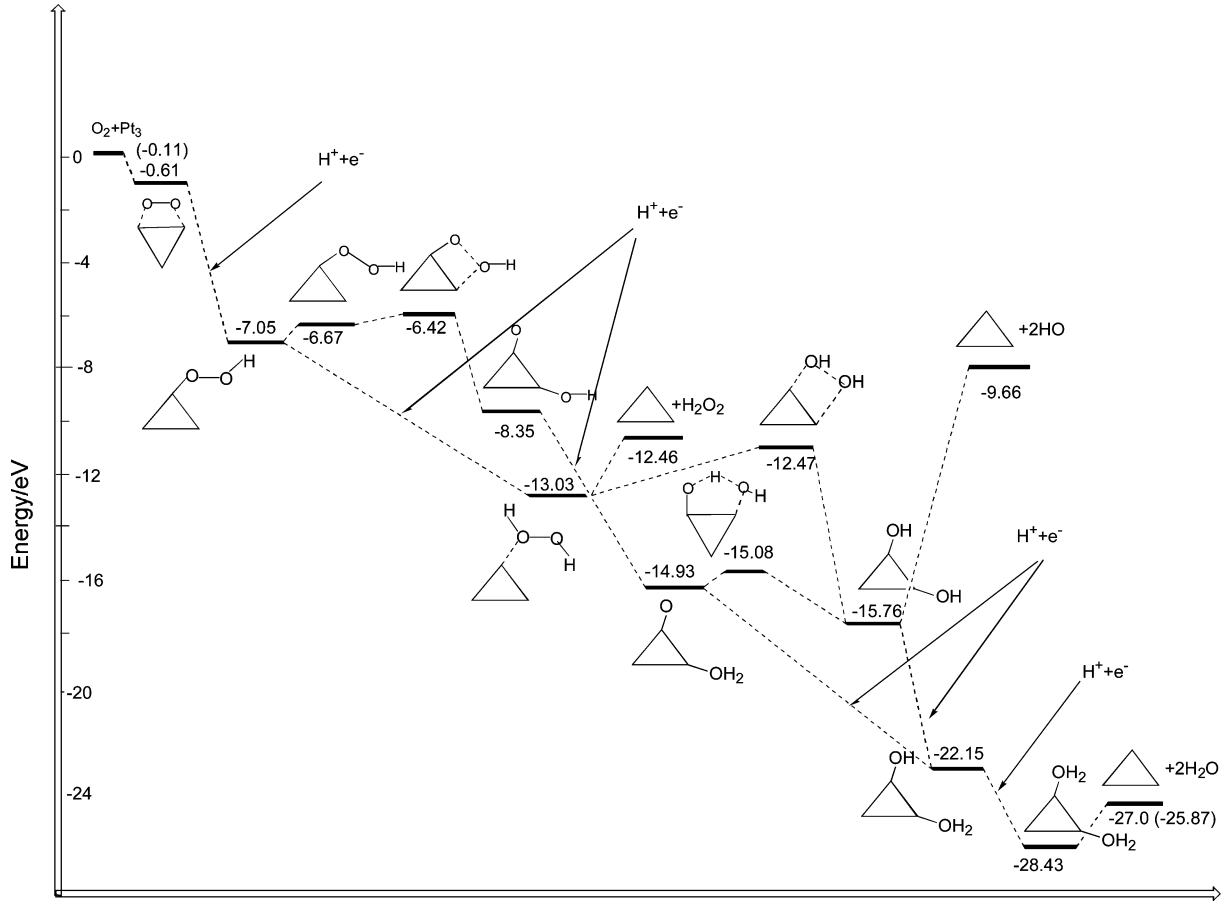

Figure 4. Potential energy surface profile for the oxygen reduction reaction: the proton was modeled by two shells of water molecules, $H^+OH_2(H_2O)_3$ $(H_2O)_6$, and the data in parentheses are Gibbs free energies.

Chart 1

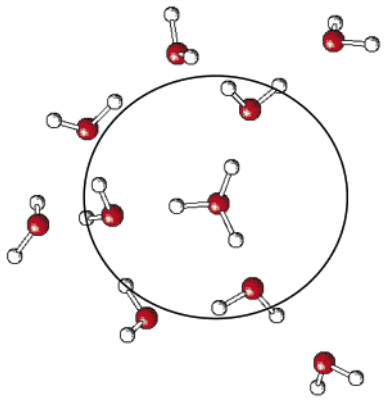

Here the proton was modeled with a hydronium solvated by three water molecules, $H^+OH_2(H_2O)_3$ (model 1), and a hydronium solvated by two shells of water molecules, H^+-$OH_2(H_2O)_3$ $(H_2O)_6$ (model 2, Chart 1), respectively. As shown in Table 3, the Gibbs energy variations for the $O_2 + 4H^+ + 4e^- = 2H_2O$ predicted by the two proton models are -29.8 and -25.9 eV. The former is too negative, while the latter gives a reversible potential of 1.87 V at the standard hydrogen scale. To get accurate values for the reversible potential of the ORR, further considerations such as bulk solvent and counterion effects are required. Table 3 shows that calculations with the MP2/6-311++G** method only slightly changes ΔG, as compared with B3LYP/6-311++G**. However, the effect of the basis set used at MP2/6-31G** is significant, e.g., increasing ΔG of the ORR by 2.5 eV for model 1, and MP2/6-31G** occasionally gives better predictions for the reversible potential of the ORR. Using such an increase to scale the ΔG at B3LYP/6-311++G** for model 2

$$\begin{aligned}\Delta G\,(\text{MP2/6-31G**, model 2}) \approx{}& \Delta G(\text{B3LYP/6-311++}\\ &\text{G**, model 2}) + \Delta G(\text{MP2/6-31G**, model 1}) - \Delta G\\ &(\text{B3LYP/6-311++G**, model 1})\\ ={}& -25.87 + (-27.3 + 29.83)\ \text{eV}\\ ={}& -23.4\ \text{eV} \qquad (1)\end{aligned}$$

The reversible potential of the ORR at the standard hydrogen scale yielded by eq 1 is 1.24 V, which is rather close to the experimental value (1.23 V) because of error cancellations hidden behind the model chemistry used.

Our previous CPMD simulations show that O_2 adsorbed on a Pt surface does not dissociate before the proton transfer, i.e., the formation of adsorbed OOH,[10,27] indicating that dissociation of adsorbed O_2 may have a higher activation energy than the formation of adsorbed OOH. This supports the speculation of Anderson et al.[6] Thus, it is assumed that adsorbed O_2 is reduced into adsorbed OOH (**S1**) in the first reduction step. Figure 4 shows that **S1** may isomerize into **S2,** and the latter decomposes into atomic oxygen and hydroxyl radical on Pt_3 (**S3**) with an activation barrier of 0.25 eV via a transition state (**TS1**). In the second reduction

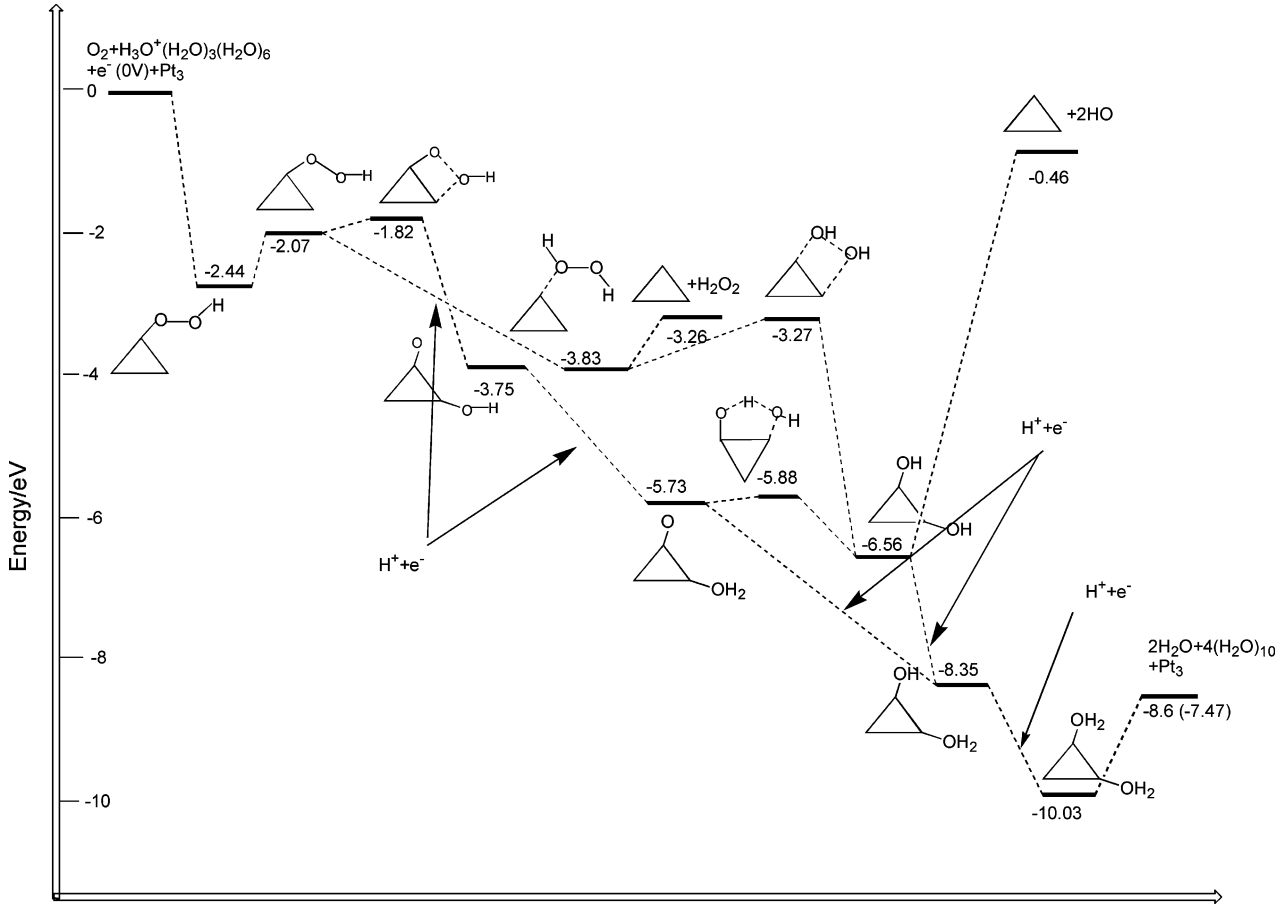

Figure 5. Potential energy surface profile for the oxygen reduction reaction at the standard hydrogen electrode potential scale: the proton was modeled by two shells of water molecules, $H^+OH_2(H_2O)_3$ $(H_2O)_6$, and the data in parentheses are Gibbs free energies.

Table 3. Reaction Energies without and with Zero Point Energy Correction (ΔE and ΔE_0, eV), Enthalpy (ΔH, eV), and Gibbs Free Energy (ΔG, eV) at 298.2 K Calculated with B3LYP

	$H_3O^+(H_2O)_3$			$H_3O^+(H_2O)_3(H_2O)_6$		
reactions	ΔE	ΔE_0	ΔG	ΔE	ΔE_0	ΔG
$O_2 + Pt_3 \rightarrow Pt_3{-}O_2$	−0.61	−0.56	−0.11	−0.61	−0.56	−0.11
$Pt_3{-}O_2 + H^+(aq) + e^- \rightarrow Pt_3{-}OOH$	−7.05	−7.03	−7.05	−6.44	−6.28	−6.06
$Pt_3{-}OOH + H^+(aq) + e^- \rightarrow Pt_3{-}O_2H_2$	−6.59	−6.57	−6.55	−5.98	−5.82	−5.56
$Pt_3{-}O_2H_2 + H^+(aq) + e^- \rightarrow HO{-}Pt_3{-}H_2O$	−9.73	−9.74	−9.74	−9.12	−8.99	−8.75
$HO{-}Pt_3{-}H_2O + H^+(aq) + e^- \rightarrow Pt_3{-}2H_2O$	−6.89	−6.86	−6.84	−6.28	−6.11	−5.85
$Pt_3{-}2H_2O \rightarrow Pt_3 + 2H_2O$	+1.46	+1.27	+0.46	+1.46	+1.27	+0.46
$O_2{+}4H^+(aq) + 4e^- \rightarrow 2H_2O$	−29.4	−29.5	−29.83	−27.0	−26.49	−25.87
$O_2{+}4H^+(aq) + 4e^- \rightarrow 2H_2O$[a]	−28.5	−28.9	−29.32			
$O_2{+}4H^+(aq) + 4e^- \rightarrow 2H_2O$[b]	−27.4	−27.3	−27.3	−25.0		−23.37[c]

[a] MP2/6-311++G**. [b] MP2/6-31G**. [c] −25.87 +(ΔG, MP2/6-31G** - ΔG, B3LYP/6-311++G**) for the model of $H_3O^+(H_2O)_3$.

step **S3** gets reduced to form coadsorbed atomic oxygen and water (**S6**). This pathway is usually referred to as a *direct* one, implying the absence of H_2O_2 in the reaction pathway. Another possibility of the second reduction step is that **S1** and/or **S2** is directly reduced by one electron to yield 1-fold adsorbed hydrogen peroxide H_2O_2 (**S4**), which can readily decompose into two coadsorbed hydroxyls (**S5**) with an activation energy barrier of 0.57 eV via the transition state (**TS2**). The pathway giving rise to H_2O_2 is usually called a *series*.

Location of one-end adsorbed hydrogen peroxide H_2O_2 (**S4**), arising from reduction of adsorbed OOH, suggests that the ORR can proceed via a *series* pathway. On the other hand, the relatively low energy barrier for the decomposition of **S2** and the high stability of **S3** in comparison with **S1** show that the end-on chemisorption precursor (**S2**) has a strong tendency to decompose before the second electron transfer. In addition, the energy of S4, ∼1.9 eV higher than S6, thermodynamically indicates that the *direct* pathway is more favorable. Therefore, although the one-end adsorbed H_2O_2 has been found, the second electron transfer step of the ORR should dominantly start with the coadsorbed O and OH (**S3**). Thus, it is theoretically validated that the O_2 reduction on a Pt(111) surface may proceed via a *parallel* pathway with the *direct* as the dominant step.

A proton transfer can occur on **S6** with an activation energy of 0.15 eV via the transition state **TS3**. Before the proton-transfer reaction, further reduction of S6 could not be excluded, which is dependent on its lifetime as well as on the competition between the proton transfer and reduction. However, intramolecular proton transfer may be more favorable than the reduction reaction involving one electron and one proton transfer.

Of the three species (**S4**, **S5**, and **S6)** from the second reduction step, **S5** (coadsorbed hydroxyls on Pt_3) is the most stable thermodynamically, followed by **S6** (coadsorbed atomic oxygen and H_2O), and **S4** (atop adsorbed H_2O_2) the least stable. H_2O_2 has quite a low adsorption energy of -0.63 eV on Pt_3, and -0.4 eV on Pt_{10}, which may enable H_2O_2 to desorb into the electrolyte phase. HO radicals are strongly adsorbed on Pt_3 with an adsorption energy of -2.61 eV per OH in **S5**. It may be speculated that OH can block active sites of Pt surface, unless OH is further reduced. Adsorbed O in S3 and S6 has the same problem due to even stronger adsorption. However, its higher reduction potential may first induce its reduction into OH.

4. Conclusions

Adsorption and decomposition of the radical OOH and H_2O_2 on Pt clusters (Pt_3, Pt_4, Pt_6, and Pt_{10}) have been extensively investigated using B3LYP type of density functional theory. Adsorption and coadsorption on Pt_3 of other relevant oxide products of the ORR have been investigated, and a potential energy surface profile for the complete reduction of oxygen in acid media has been proposed. The OOH radical has a very strong adsorption on Pt clusters. Both thermodynamics and kinetics indicate that OOH readily decomposes into O and OH before a second electron transfer takes place. Thus, although a one-end adsorbed hydrogen peroxide H_2O_2, arising from the reduction of adsorbed OOH, has also been located on Pt_3 and Pt_{10}, a favorable pathway for the second electron transfer should occur on the coadsorbed O and OH species, suggesting that O_2 reduction on a Pt surface may proceed via a *parallel* pathway: the *direct* (no H_2O_2 generated as intermediate) and *series* (H_2O_2 generated) occurring simultaneously, with the *direct* as the dominant step.

Acknowledgment. Financial support from the Department of Energy/Basic Energy Sciences, (DE-FG02-04ER15619) and from DURIP/ARO (Grant No. W911N F-04-1-0098) is gratefully acknowledged. The use of computational facilities at the NSF HPC and TeraGrid Sites: National Center for Supercomputing Applications (CHE040052) is appreciated.

References

(1) Damjanovic, A.; Brusic, V. Electrode kinetics of oxygen reduction on oxide-free platinum electrodes. *Electrochim. Acta* **1967**, *12*, 615−628.

(2) Yeager, E. B. Electrocatalysts for O_2 reduction. *Electrochim. Acta* **1984**, *29*, 1527−1537.

(3) Adzic, R. R.; Wang, J. X. Configuration and site of O_2 adsorption on the Pt(111) electrode surface. *J. Phys. Chem. B* **1998**, *102*, 8988−8993.

(4) Markovic, N. M.; Ross, P. N. Surface science studies of model fuel cell electrocatalysts. *Surf. Sci. Rep.* **2002**, *45*, 117−229.

(5) Anderson, A. B.; Albu, T. V. Catalytic effect of platinum on oxygen reduction: An ab initio model including electrode potential dependence. *J. Electrochem. Soc.* **2000**, *147*, 4229−4238.

(6) Sidik, R. A.; Anderson, A. B. Density functional theory study of O_2 electroduction when bonded to a Pt dual site. *J. Electroanal. Chem.* **2002**, *528*, 69−76.

(7) Murthi, V. S.; Urian, R. C.; Mukerjee, S. Oxygen reduction kinetics in low and medium-temperature acid environment: Correlation of water activation and surface properties in supported Pt and Pt alloy electrocatalysts. *J. Phys. Chem. B* **2004**, *108*, 11011−11023.

(8) Steele, B. C. H.; Heinzel, A. Materials for fuel-cell technologies. *Nature* **2001**, *414*, 345−352.

(9) Markovic, N. M.; Schmidt, T. J.; Stamenkovic, V.; Ross, P. N. Oxygen reduction reaction on Pt and Pt bimetallic surfaces: A selective review. *Fuel Cells* **2001**, *1*, 105−116.

(10) Wang, Y.; Balbuena, P. B. Ab initio-molecular dynamics studies of O_2 electroreduction on Pt (111): Effects of proton and electric field. *J. Phys. Chem. B* **2004**, *108*, 4376−4384.

(11) Stamenkovic, V.; Schmidt, T. J.; Ross, P. N.; Markovic, N. M. Surface composition effects in electrocatalysis: Kinetics of oxygen reduction on well-defined Pt_3Ni and Pt_3Co alloy surfaces. *J. Phys. Chem. B* **2002**, *106*, 11970−11979.

(12) Nakanishi, S.; Mukouyama, Y.; Karasumi, K.; Imanishi, A.; Furuya, N.; Nakato, Y. Appearance of oscillation through the autocatalytic mechanism by control of the atomic-level structure of electrode surfaces in electrochemical H_2O_2 reduction at Pt electrodes. *J. Phys. Chem. B* **2000**, *104*, 4181−4188.

(13) Balbuena, P. B.; Altomare, D.; Vadlamani, N.; Bingi, S.; Agapito, L. A.; Seminario, J. M. Adsorption of O, OH, and H_2O on Pt-based bimetallic clusters alloyed with Co, Cr, and Ni. *J. Phys. Chem. A* **2004**, *108*, 6378−6384.

(14) Panchenko, A.; Koper, M. T. M.; Shubina, T. E.; Mitchell, S. J.; Roduner, E. Ab initio calculations of intermediates of oxygen reduction on low-index platinum surfaces. *J. Electrochem. Soc.* **2004**, *151*, A2016−A2027.

(15) Li, T.; Balbuena, P. B. Computational studies of the interactions of oxygen with platinum clusters. *J. Phys. Chem. B* **2001**, *105*, 9943−9952.

(16) Balbuena, P. B.; Altomare, D.; Agapito, L. A.; Seminario, J. M. Adsorption of oxygen on Pt-based clusters alloyed with Co, Ni, and Cr. *J. Phys. Chem. B* **2003**, *107*, 13671−13680.

(17) Jacob, T.; Muller, R. P.; W. A. Goddard, I. Chemisorption of atomic oxygen on Pt(111) from DFT studies of Pt-clusters *J. Phys. Chem. B* **2003**, *107*, 9465−9476.

(18) Becke, A. D. A new mixing of Hartree−Fock and local density-functional theories. *J. Chem. Phys.* **1993**, *98*, 1372−1377.

(19) Lee, C.; Yang, W.; Parr, R. G. Development of the Colle-Salvetti correlation-energy formula into a functional of the electron density. *Phys. Rev. B* **1988**, *37*, 785−789.

(20) Frisch, M. J.; Trucks, G. W.; Schlegel, H. B.; Scuseria, G. E.; Robb, M. A.; Cheeseman, J. R.; Montgomery, J. A.; Vreven, T.; Kudin, K. N.; Burant, J. C.; Millam, J. M.; Iyengar, S. S.; Tomasi, J.; Barone, V.; Mennucci, B.; Cossi, M.; Scalmani, G.; Rega, N.; Petersson, G. A.; Nakatsuji, H.; Hada, M.; Ehara, M.; Toyota, K.; Fukuda, R.; Hasegawa, J.; Ishida, M.; Nakajima, T.; Honda, Y.; Kitao, O.; Nakai,

H.; Klene, M.; Li, X.; Knox, J. E.; Hratchian, H. P.; Cross, J. B.; Bakken, V.; Adamo, C.; Jaramillo, J.; Gomperts, R.; Stratmann, R. E.; Yazyev, O.; Austin, A. J.; Cammi, R.; Pomelli, C.; Ochterski, J. W.; Ayala, P. Y.; Morokuma, K.; Voth, G. A.; Salvador, P.; Dannenberg, J. J.; Zakrzewski, V. G.; Dapprich, S.; Daniels, A. D.; Strain, M. C.; Farkas, O.; Malick, D. K.; Rabuck, A. D.; Raghavachari, K.; Foresman, J. B.; Ortiz, J. V.; Cui, Q.; Baboul, A. G.; Clifford, S.; Cioslowski, J.; Stefanov, B. B.; Liu, G.; Liashenko, A.; Piskorz, P.; Komaromi, I.; Martin, R. L.; Fox, D. J.; Keith, T.; Al-Laham, M. A.; Peng, C. Y.; Nanayakkara, A.; Challacombe, M.; Gill, P. M. W.; Johnson, B.; Chen, W.; Wong, M. W.; Gonzalez, C.; Pople, J. A. Gaussian03; Revision C.02 ed.; Gaussian, Inc.: Wallingford, CT, 2004.

(21) Wadt, W. R.; Hay, P. J. Ab initio effective core potentials for molecular calculations. Potentials for main group elements Na to Bi. *J. Chem. Phys.* **1985**, *82*, 284−298.

(22) Boys, S. F.; Bernardi, F. Calculations of small molecular interactions by differences of separate total energies. Some procedures with reduced errors. *Mol. Phys.* **1970**, *19*, 553.

(23) Majumdar, D.; Dai, D.; Balasubramanian, K. Theoretical study of the electronic states of platinum trimer (Pt_3) *J. Chem. Phys.* **2000**, *113*, 7919−7927.

(24) Michaelides, A.; Hu, P. A density functional theory study of hydroxyl and the intermediate in the water formation reaction on Pt. *J. Chem. Phys.* **2001**, *114*, 513−519.

(25) Stamenkovic, V.; Grgur, B. N.; Ross, P. N.; Markovic, N. M. Oxygen reduction reaction on Pt and Pt-bimetallic electrodes covered by CO − Mechanism of the air bleed effect with reformate. *J. Electrochem. Soc.* **2005**, *152*, A277−A282.

(26) Kim, D.-H.; Lee, B.-K.; Lee, D. S. Determination of trace anions in concentrated hydrogen peroxide by direct injection ion chromatography with conductivity detection after Pt-catalyzed on-line decomposition. *Bull. Korean Chem. Soc.* **1999**, *20*, 696−700.

(27) Wang, Y.; Balbuena, P. B. Ab initio molecular dynamics simulations of the oxygen electroreduction reaction on a Pt(111) surface in the presence of hydrated hydronium $(H_3O)+(H_2O)_2$: Direct or series pathway? *J. Phys. Chem. B*, in press.

(28) Gland, J. L. Molecular and atomic adsorption of oxygen on the Pt (111) and Pt (S)-12 (111) x (111) surfaces. *Surf. Sci.* **1980**, *93*, 487−514.

(29) Anderson, A. B.; Albu, T. V. Ab Initio Determination of Reversible Potentials and Activation Energies for Outer-Sphere Oxygen Reduction to Water and the Reverse Oxidation Reaction. *J. Am. Chem. Soc.* **1999**, *121*, 11855−11863.

CT0500794